The Crystal Structures, Magnetic and Electrical Properties of Two Polymeric Chlorocuprate(II) Compounds†

Luigi Pietro Battaglia and Anna Bonamartini Corradi
Istituto di Chimica Generale ed Inorganica, Centro di Studio per la Strutturistica Diffrattometrica del C.N.R., University of Parma, Via D'Azeglio 85, 43100 Parma, Italy
Urs Geiser and Roger D. Willett
Department of Chemistry, Washington State University, Pullman, WA 99164, U.S.A.
Antonio Motori and Franco Sandrolini
Istituto Chimico, Facoltà di Ingegneria, University of Bologna, Viale Risorgimento 2, 40136 Bologna, Italy
Luciano Antolini, Tiziano Manfredini, Ledi Menabue, and Gian Carlo Pellacani*
Dipartimento di Chimica, University of Modena, Via Campi 183, 41100 Modena, Italy

The crystal structures of piperidinium trichlorocuprate(II) [Hpip][$CuCl_3$], and piperazinium hexachlorodicuprate(II), [H_2pipz][Cu_2Cl_6], have been determined by *X*-ray diffraction techniques. [Hpip][$CuCl_3$] is monoclinic, space group $C2/c$, with a = 18.385(7), b = 8.439(4), c = 11.878(5) Å, and β = 103.63(5)° while [H_2pipz][Cu_2Cl_6] is triclinic, $P\bar{1}$, with a = 7.984(4), b = 7.054(4), c = 6.104(3) Å, α = 111.23(8), β = 99.95(9), γ = 81.26(7)°. Both salts contain infinite chains of $[Cu_2Cl_6]^{2-}$ dimers. The $[Cu_2Cl_6]^{2-}$ dimers show significant distortions from planarity due to formation of semi-co-ordinate bonds between adjacent dimers, with a larger distortion for the Hpip salt. This bifold distortion gives each copper(II) ion a (4 + 1) co-ordination geometry. The chains have slightly different configurations. In the H_2pipz salt, adjacent dimers are related by unit-cell translations, while in the Hpip salt they are related by a *c*-glide operation. Magnetic susceptibility measurements show that the H_2pipz salt is an alternating antiferromagnetic chain with J/k = −13.35(7) K and J'/k = −7.6(3) K, while the Hpip salt is an alternating ferro- antiferro-magnetic chain with J/k = 26(3) K and J'/k = −0.24(1) K. Thus, the intradimer coupling (J) becomes less antiferromagnetic as the distortion from planarity increases. Comparison with other bifolded dimers confirms correlation of J with the bifold angle, both experimentally and theoretically. Electrical measurements reveal the presence of an activated process for electrical conduction with activation parameters of 0.44 eV for [Hpip][$CuCl_3$] and 0.34 eV for [H_2pipz][Cu_2Cl_6]. The charge carriers are proposed to be the protons in N–H · · · Cl hydrogen bonds.

The primary interest in the halogenocuprates(II) derives simply from the fact that they are able to assume, with great ease, very different geometries. Among the factors upon which this characteristic depends are the Jahn–Teller effect, crystal field stabilization, ligand–ligand repulsion, shape and size of the counter ions, van der Waals forces, and hydrogen-bonding interactions.[1] In our laboratories, it has been shown that the co-ordination geometries can be systematically varied through the judicious choice of organic counter ions and that, based on the size, shape, and hydrogen-bonding capabilities, it is possible to predict the stereochemistry to some extent. The use of substituted piperidinium and piperazinium cations has produced a wide range of structural properties.[2] In $[A]_2[CuCl_4]$ salts, the stereochemistry of the $[CuCl_4]^{2-}$ ions ranges from square planar to nearly tetrahedral. It has been possible to correlate this with the hydrogen-bonding ability of the organic counter ion.[3] Similar results are seen for $[A]_2[CuBr_4]$ salts.[4] The effect of these various factors listed above upon the structures of [A][$CuCl_3$] salts has recently been reviewed.[5] In addition, copper(II) halides have played an important role in the development of magneto-structural correlations[6] and the development of low-dimensional magnetism,[7] in catalytic processes,[8] spectroscopic properties of copper(II) proteins,[9] and thermochromism.[10a]

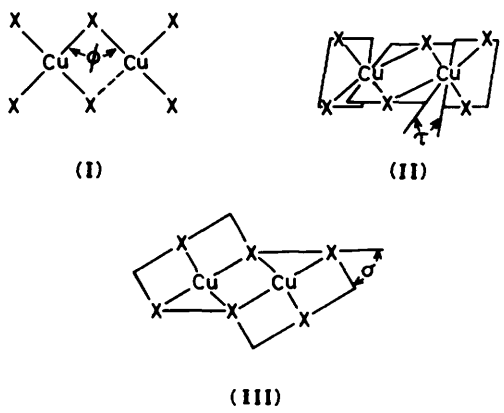

Figure 1. Examples of the stereochemistry of the dimeric species: (**I**) planar, (**II**) twisted, (**III**) bifolded forms

For species of a stoicheiometry [A][CuX_3], where X = Cl or Br and A is an organic or inorganic cation, it is possible to subdivide the compounds into three general classes:[5] (i) isolated $[Cu_nX_{3n}]^{n-}$ oligomers,‡ (ii) stacked $[Cu_2X_6]^{2-}$ dimers, (iii) linear chains. Examples of the stereochemistry of the dimeric species include planar (**I**), twisted (**II**), and chair or bifolded forms (**III**) (Figure 1). The isolated dimers usually form the

† *Supplementary data available* (No. SUP 56679, 7 pp.): loss factor and dielectric constant plots, and charging and discharging current plots. See Instructions for Authors, *J. Chem. Soc., Dalton Trans.*, 1988, Issue 1, pp. xvii—xx.

Non-S.I. unit employed: eV ≈ 1.60 × 10^{-19} J.

‡ In ref. 3, this class contains only $[Cu_2X_6]^{2-}$ dimers. However, we have recently shown[10b] that $[NEt_4][CuCl_3]$ contains isolated $[Cu_4Cl_{12}]^{4-}$ tetrameric units.

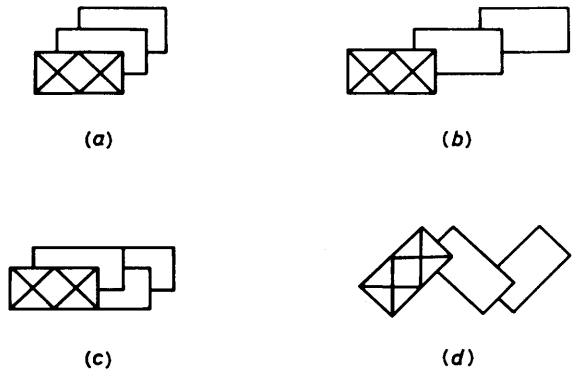

Figure 2. Stacking patterns for quasi-planar $[Cu_2Cl_6]^{2-}$ dimers: (*a*) $K[CuCl_3]$, (*b*) $[H_2pipz][Cu_2Cl_6]$, (*c*) $[H_2tatz][Cu_2Cl_6]$, (*d*) [Hpip]-$[CuCl_3]$

twisted type (**II**), although two salts with a planar arrangement have recently been reported.[11] Various arrangements and extents of distortion of these dimers are possible. As examples, the planar (**I**) and chair (**III**) forms of the dimers form stacks with a semi-co-ordinated Cu–X linkage between stacks, giving each copper(II) ion a (4 + 1) or (4 + 2) co-ordination geometry. Such interactions lead to a variety of stacking patterns,[12,13] as illustrated schematically in Figure 2.

In this paper we report on the structural, magnetic, and electrical properties of the copper(II) trichloride salts with the piperidinium(1+) (Hpip) and piperazinium(2+) (H_2pipz) cations. The structures are very similar to other so-called 'bifolded' dimer salts in the $[A][CuCl_3]$ series[14] and we will correlate their magnetic properties with those previously reported.

Experimental

Preparation of Complexes.—Piperidinium trichlorocuprate(II). This salt was precipitated by the evaporation of an alcoholic solution (methanol, ethanol, Pr^nOH) containing piperidinium chloride and copper(II) chloride dihydrate in a molar ratio of 1:2 (Found: C, 23.45; H, 4.90; N, 5.45. Calc. for $C_5H_{11}Cl_3CuN$: C, 23.45; H, 4.70; N, 5.45%).

Piperazinium hexachlorodicuprate(II). This salt was prepared by the evaporation of a mixture of piperazine dihydrochloride and $CuCl_2{\cdot}2H_2O$ (1:4 molar ratio) in concentrated hydrochloric acid (Found: C, 11.65; H, 2.85; N, 6.70. Calc. for $C_4H_{12}Cl_6Cu_2N_2$: C, 11.20; H, 2.85; N, 6.55%).

Magnetic Measurements.—Susceptibility measurements were made on a PAR model 155 vibrating sample magnetometer at Washington State University equipped with a Janis model 153 flow-through cryostat using a home-built magnet, with magnetic field strengths up to 10 kOe (Oe = $1\,000/4\pi$ A m^{-1}), and calibrated Hall probe. Temperature was measured with a germanium resistance thermometer calibrated against potassium chrome alum $[K_2Cr_2(SO_4)_4{\cdot}24H_2O]$ and $Hg[Co(SCN)_4]$.[15] In the liquid nitrogen range, a thermocouple using the calibration given by the National Bureau of Standards[16] was used. Diamagnetic corrections and temperature-independent paramagnetism corrections were made.

Electrical Measurements.—Sample preparation. The compound $[Hpip][CuCl_3]$ was finely powdered by hand, dried to constant weight at 25 °C and stored in the dark, under vacuum over P_2O_5 until electrical measurements were made. The compound $[H_2pipz][Cu_2Cl_6]$ showed some inclusion of hydrochloric acid in its crystals. It was, therefore, finely powdered by hand, dried to constant weight at 50 °C under dynamic vacuum and in the presence of KOH for 3 d, after which the hydrochloric acid appeared to be completely removed (thermogravimetrically controlled), and finally stored in the dark, under vacuum over P_2O_5 until required for electrical measurements. Discs (diameter 28 mm and thickness *ca.* 1—2 mm) suitable for the electrical measurements were prepared from the powders by compaction (under vacuum) at a pressure of 0.2 kN mm^{-2}. Samples were then sintered under vacuum for 10 h at 110 °C for $[Hpip][CuCl_3]$ and 120 °C for $[H_2pipz][Cu_2Cl_6]$, the sintering temperatures being chosen according to the previously ascertained thermal stabilities under vacuum of the compounds by differential thermal analysis and differential scanning calorimetry measurements.

Measurement techniques. Preliminary measurements showed the somewhat low electrical conductivities of the compounds at room temperature. The electrical measurements were therefore performed by a three-terminal technique. Voltmeter–ammeter method, in d.c. (direct current), and Schering bridge method, in a.c. (alternating current), measurements were used (cells and instrumentation described elsewhere[12,17–19]) to determine both dielectric relaxation processes and electrical conductivity in the samples. The samples were then coated with gold by vacuum deposition. Electrical measurements were made in dynamic vacuum from sintering to room temperature, to minimize the effects of casual adsorption of gases or vapours on the sample surfaces. No structural change was revealed after electrical measurements by *X*-ray investigations. D.c. charging currents were measured under an electrical field of 1 kV cm^{-1}.

Table 1. Crystal data for $[Hpip][CuCl_3]$ and $[H_2pipz][Cu_2Cl_6]$

Formula	$C_{10}H_{22}Cl_6Cu_2N_2$	$C_4H_{12}Cl_6Cu_2N_2$
M	496.0	428.0
Space group	$C2/c$	$P\bar{1}$
a/Å	18.385(7)	7.984(4)
b/Å	8.439(4)	7.054(4)
c/Å	11.878(5)	6.104(3)
α/°	90.0	111.23(8)
β/°	103.63(5)	99.95(9)
γ/°	90.0	81.26(7)
U/Å^3	1 791(1)	314.1(3)
Z	4	1
D_m/g cm^{-3}	1.85	2.27
D_c/g cm^{-3}	1.84	2.26
μ(Mo-K_α)/cm^{-1}	32.77	46.5
$F(000)$	968	210
Crystal size (mm)	0.25 × 0.31 × 0.41	0.26 × 0.36 × 0.48
Diffractometer	Philips PW1100	Philips PW1100
Absorption correction (min.—max.)*	1.00—1.34	1.00—2.16
Scan speed (° min^{-1})	4.8	6.0
Scan width (°)	2.0	1.8
Radiation (λ/Å)	Mo-K_α (0.710 69)	Mo-K_α (0.710 69)
θ range (°)	3—24	2.5—25
Standard reflection every	60 min	60 min
Intensity variation (max.)	2.3%	4.5%
Scan mode	ω—2θ	ω—2θ
No. of measured reflections	1 596	1 103
Condition for observation	$I > 3\sigma(I)$	$I > 3\sigma(I)$
No. of observed reflections	1 151	949
No. of parameters refined	127	64
$R = \Sigma\|\Delta F\|/\Sigma\|F_o\|$	0.0243	0.0643
$R' = \|w(\Delta F)^2/\Sigma wF_o^2\|^{\frac{1}{2}}$	0.0282	0.0666
k, g in $w = k/[\sigma^2(F_o) + gF_o^2]$	1, 0.0008	1, 0.000 05

* Absorption correction applied by ψ-scan technique (A.C.T. North, D. C. Phillips, and F. S. Mathews, *Acta Crystallogr., Sect. A*, 1968, **24**, 351).

Also, discharging currents were measured by shorting electrodes to detect possible relaxation effects in the ultra-low-frequency range.[20]

X-*Ray Crystallography*.—In both compounds unit-cell parameters and intensity data were measured on a Philips PW 1100 single-crystal automatic diffractometer[21] with the samples randomly oriented. Cell parameters and their e.s.d.s were refined by a least-squares method from the accurate positioning of 20 strong reflections for [Hpip][$CuCl_3$] and 25 for [H_2pipz][Cu_2Cl_6]. Crystal data and structural details are reported in Table 1. Intensities, corrected for Lorentz polarization and absorption effects, were put on an absolute scale by least-squares analysis. Both structures were solved by the heavy-atom technique: the copper atoms were located by combining Patterson and Fourier methods. The resulting Fourier syntheses gave the positions of all non-hydrogen atoms. The refinement was carried out isotropically and anisotropically by least-squares minimization of the function $\Sigma w|\Delta F|^2$ using the weighting scheme $w^{-1} = \sigma^2 F_o + gF_o^2$.

In [Hpip][$CuCl_3$], after anisotropic refinement of Cu, Cl, N, and C, the hydrogen atoms were located in a ΔF map and introduced in the refinement with isotropic thermal parameters 1.0 Å^2 higher than the bonded atoms. Further refinement of this model, carried out with anisotropic thermal parameters for Cu, Cl, N, and C, led to final convergence at $R = 0.0243$ and $R' = 0.0282$. In [H_2pipz][Cu_2Cl_6], after anisotropic refinement of Cu, Cl, N, and C, the hydrogen atoms were located in a ΔF map and introduced in the final structure factor calculation with isotropic thermal parameters. In this way the final R index was determined to be 0.0643 and $R' = 0.066$. Atomic scattering factors were taken from the International Tables; both real and imaginary components of anomalous dispersion were included.[22] Final atomic co-ordinates of non-hydrogen atoms are quoted in Table 2.

All calculations were performed using a CYBER 76 computer of the Centro di Calcolo Interuniversitario dell'Italia Nord-Orientale, Bologna, with the financial support of the University of Parma, using the SHELX system of programs.[23]

Table 2. Final atomic co-ordinates with e.s.d.s in parentheses

Atom	*x*	*y*	*z*
(*a*) [Hpip][$CuCl_3$]			
Cu	0.026 42(2)	0.117 59(4)	0.118 21(3)
Cl(1)	−0.044 47(5)	0.138 63(9)	−0.066 90(7)
Cl(2)	0.093 22(4)	0.086 54(9)	0.301 00(7)
Cl(3)	0.055 74(5)	0.376 62(8)	0.120 13(7)
N	0.107 3(2)	0.505 8(4)	0.386 8(3)
C(1)	0.117 4(2)	0.667 9(5)	0.349 2(4)
C(2)	0.180 3(2)	0.675 2(5)	0.291 3(4)
C(3)	0.249 9(2)	0.605 3(5)	0.364 7(4)
C(4)	0.236 7(3)	0.442 3(5)	0.403 9(5)
C(5)	0.174 2(2)	0.441 2(5)	0.463 0(4)
(*b*) [H_2pipz][Cu_2Cl_6]			
Cu	0.093 5(2)	−0.059 9(1)	0.245 7(1)
Cl(1)	0.155 0(2)	0.118 3(3)	0.648 6(3)
Cl(2)	−0.027 2(2)	0.265 5(3)	0.135 3(3)
Cl(3)	0.376 1(2)	−0.101 6(3)	0.207 8(3)
N	0.418 0(8)	0.686 3(9)	0.648 9(10)
C(1)	0.312 0(10)	0.522 1(11)	0.470 3(13)
C(2)	0.586 9(10)	0.597 3(11)	0.736 4(13)

Results and Discussion

Description of the Structures.—The crystal structures of both compounds contain isolated organic cations and infinite chains of [Cu_2Cl_6]$^{2-}$ dimers parallel to the respective crystallographic *c* axes. Hydrogen-bonding interactions provide stability to the lattice. Pertinent bond distances and angles are summarized in Table 3. Views of the structures of the Hpip and H_2pipz salts are given in Figures 3 and 4 respectively. The anionic portions of the structures consist of stacks of bifolded centrosymmetric [Cu_2Cl_6]$^{2-}$ dimers. In the Hpip salt, adjacent dimers are related by two-fold axes, and the chains assume the stacking patterns illustrated in Figure 2(*d*). On the other hand, adjacent dimers in the H_2pipz salt are related by unit-cell translations, and the stacking is illustrated in Figure 2(*b*). In each case, each copper atom forms a semico-ordination bond to a Cl(2) atom in the adjacent dimer with a concomitant distortion of the

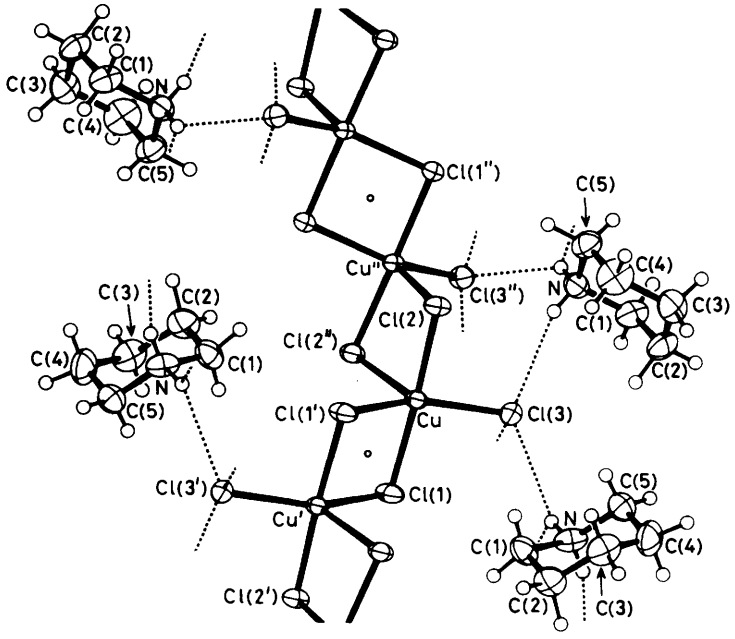

Figure 3. The crystal structure of piperidinium trichlorocuprate(II). The *c* axis is vertical

geometry in the basal plane, the distortions being larger in the Hpip salt. Thus, the smallest *trans* Cl–Cu–Cl bond angle is 150.43(4)° in the Hpip salt and 156.8(1)° in the H_2pipz salt. The equatorial Cu–Cl bond lengths are considerably shorter for the Hpip salt [2.267(2) (average) *vs.* 2.298(3) Å for H_2pipz] but the axial semico-ordinate distances are virtually identical [2.612(1) *vs.* 2.622(3) Å]. Of interest in the discussion of magnetic properties are the intradimer bridging angles, Cu–Cl(1)–Cu′ [φ in structure (**I**), Figure 1], of 95.5(1) and 95.8(2)°, the interdimer bridging angles, Cu-Cl(2)-Cu′ (φ′) of 87.1(1) and 89.1(2)°, and the bifold angles [σ in structure (**III**), Figure 1] of 29.6 and 23.2° respectively. The semico-ordinate bond lengths are the shortest yet observed for the stacking of $[Cu_2Cl_6]^{2-}$ dimers (see Table 4). This leads to some interdimer Cl–Cl contacts which are substantially shorter than the sum of the van der Waals radii (3.6 Å): Cl(2)–Cl(2′) 3.356(2) and Cl(1)–Cl(2′) 3.508(2) Å in the Hpip salt, Cl(2)–Cl(2′) 3.496(3) Å in the H_2pipz salt. Hence, we conclude that there is a substantial admixture of trigonal-bipyramidal structure in the observed stereochemistry.[24]

The geometries of both cations are normal with, as anticipated from hydrogen-bonding considerations, greater thermal motion of the piperidinium cation than of the piperazinium cation. In both cases, the NH_2 moieties of the cations are involved in three hydrogen bonds to the non-bridging chloride ion, Cl(3), with one normal N–H ··· Cl interaction and one bifurcated hydrogen bond. The hydrogen bonds are slightly shorter in [Hpip][$CuCl_3$], since the mononitrogen base is able to adapt more readily stereochemically. The hydrogen-bonding arrangement is consistent with the concepts of electroneutrality[5] where it is argued that in polymeric structures, the halide ions will either be involved in bridge formation or hydrogen bonds in order to maximize electrostatic interactions.

Table 3. Selected bond distances (Å) and angles (°) with e.s.d.s in parentheses for the compounds

	[Hpip][$CuCl_3$]	[H_2pipz][Cu_2Cl_6]
Cu–Cl(1)	2.283(2)	2.324(3)
Cu–Cl(2)	2.244(2)	2.271(3)
Cu–Cl(3)	2.250(1)	2.272(2)
Cu–Cl(1′)	2.292(1)	2.325(2)
Cu–Cl(2′)	2.612(1)	2.622(3)
Cu–Cu′ (intra)	3.389(1)	3.442(3)
Cu–Cu″ (inter)	3.490(2)	3.450(3)
Cl(1)–Cu–Cl(2)	177.35(5)	173.1(1)
Cl(1)–Cu–Cl(3)	90.87(4)	89.9(1)
Cl(1)–Cu–Cl(1′)	84.43(4)	84.2(1)
Cl(2)–Cu–Cl(3)	91.63(4)	92.1(1)
Cl(2)–Cu–Cl(1′)	93.80(4)	91.4(1)
Cl(3)–Cu–Cl(1′)	150.43(4)	156.8(1)
Cl(1)–Cu–Cl(2′)	91.30(4)	95.0(1)
Cl(2)–Cu–Cl(2′)	87.07(4)	90.9(1)
Cl(3)–Cu–Cl(2′)	108.32(4)	104.8(4)
Cl(1′)–Cu–Cl(2′)	100.98(4)	98.1(1)
Cu–Cl(1)–Cu′	95.5(1)	95.8(2)
Cu–Cl(2)–Cu′	87.1(1)	89.1(2)

Magnetic Interactions.—Based on the structural results, we anticipate both salts to be characterized magnetically as alternating chains, specified by the Hamiltonian below. The

$$\mathcal{H} = -2J\Sigma(\vec{S}_{2i}\vec{S}_{2i+1} + \alpha\vec{S}_{2i+1}\vec{S}_{2i+2})$$

susceptibility of piperazinium hexachlorodicuprate(II) shows a reduced moment as compared with the Curie law, with a maximum at $T_{max.}$ = 15 K, and a drop towards zero at lower temperatures (Figure 5). This behaviour is very typical of an alternating antiferromagnetic chain for which $|J/k| \sim 0.8T_{max.}$ while α is determined by the value of χ at $T_{max.}$. The solid line is the best fit through all data using the model of Hatfield and co-workers[25] with an exchange constant $J/k = -13.35(7)$ K, alternation parameter $\alpha = 0.57(2)$ [$J'/k = -7.6(3)$ K], and $g = 2.063(7)$. The curve represents the area of the maximum very well, but at higher temperatures the measured data are somewhat too high. The larger J value is assumed to be the intradimer coupling, since this is normally expected to be larger than the interdimer coupling.

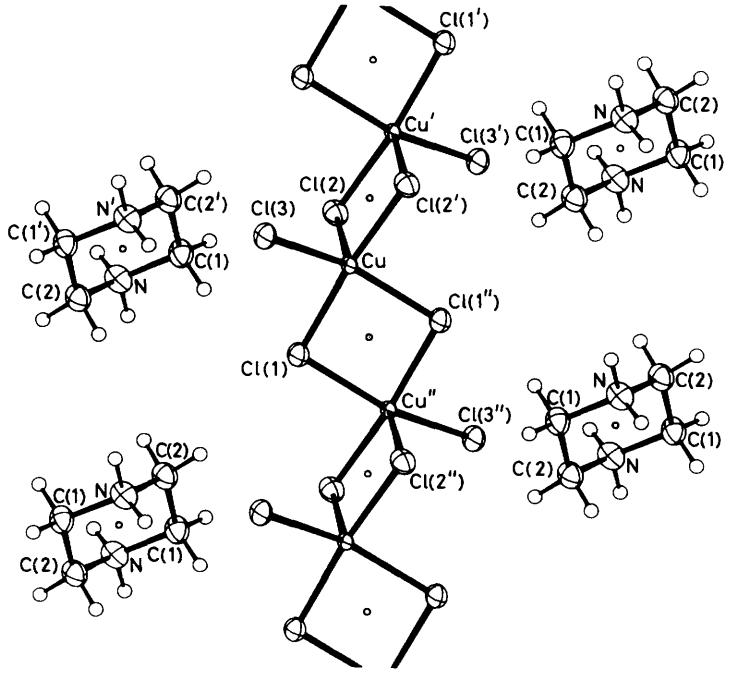

Figure 4. The crystal structure of piperazinium hexachlorodicuprate(II). The *c* axis is vertical

Table 4. Structural and magnetic data for copper chloride dimer chains

Compound	Cu–Cl–Cu′ φ(intra)/°	Cu–Cl–Cu′ φ′(inter)/°	Cu–Cl/Å (basal)	Cu–Cl/Å (axial,*r*)	φ′/*r*	Bifold σ/°	*J*/*k* K	*J*′/*k* K	($\varepsilon_s - \varepsilon_a$)/eV
$K[CuCl_3]$[a]	95.5	91.0—100.6	2.288	2.941, 3.113	—	1.5	−28	—	0.1153
$[H_2tatz][Cu_2Cl_6]$[b]	95.8	95.0	2.292	2.730, 3.125	34.8	7.6	−28	*ca.* 7	0.1140
$[NH_3Pr^i][CuCl_3]$[c]	95.5	89.4	2.290	2.699	33.1	19.5	−14	−8	0.1128
$[H_2pipz][Cu_2Cl_6]$[d]	95.8	89.1	2.298	2.622	34.0	23.2	−13	−8	0.1093
$[NH_2Me_2][CuCl_3]$[c]	95.6	91.5	2.300	2.733	33.5	24.0	15	−13	0.1018
$[Hpip][CuCl_3]$[d]	95.5	87.1	2.267	2.612	33.3	29.6	26	−0.2	0.1042
$[Hbzpip][CuCl_3]$[c]	95.2	92.9	2.290	2.669	34.3	29.0	30	−1.2	0.0914
$[H_2dmbipy][Cu_2Cl_6]$[e]	97.5	94.0	2.288	2.668	35.2	31.7	−18	<0.1	0.1111

[a] R. D. Willett, C. Dwiggens, R. F. Kruh, and R. E. Rundle, *J. Chem. Phys.*, 1963, **38**, 2429; G. J. Maass, B. C. Gerskin, and R. D. Willett, *ibid.*, 1967, **46**, 401. [b] Ref. 12. [c] Ref. 10*b*. [d] This work. [e] Ref. 8.

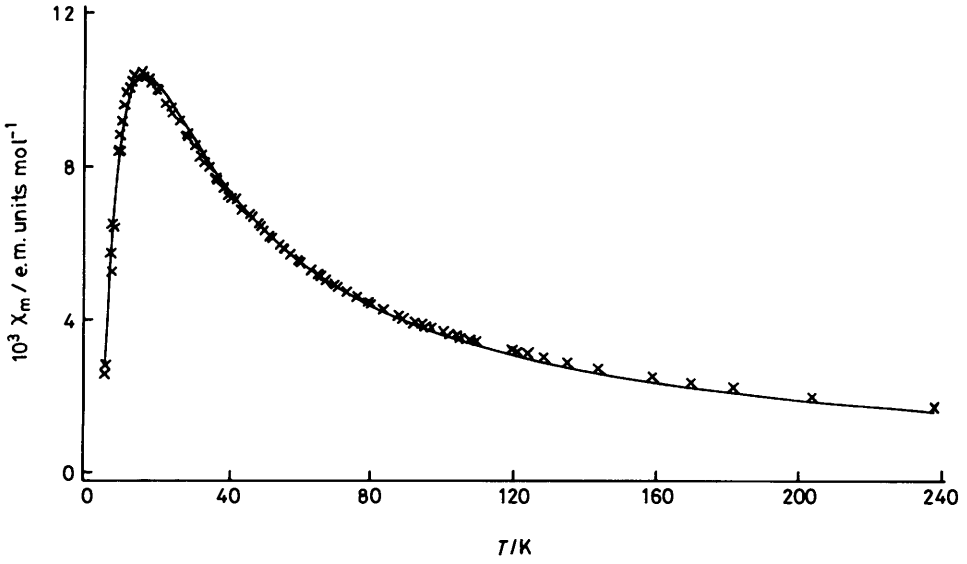

Figure 5. Molar powder susceptibility of piperazinium hexachlorodicuprate(II). (x) Observed values (per mole Cu); (——) calculated curve using $J/k = -13.35$ K, $g = 2.063$, $\alpha = J'/J = 0.57$

The susceptibility of piperidinium trichlorocuprate(II) diverges smoothly at low temperatures. A plot of χT *vs.* T is therefore shown to reveal more details (see Figure 6). Upon heating, the product χT increased by approximately 3% between 44 and 46 K. A least-squares fit of all data to a mean-field-corrected dimer model[26] produced values of $J/k = 26(3)$ K and $ZJ'/k = -0.49(1)$ K ($Z = 2$) with g fixed at 2.17. Again, the larger J value is associated with the intradimer coupling.

Magneto-structural Correlation.—Both compounds consist of chains of centrosymmetric $[Cu_2Cl_6]^{2-}$ dimers, with one of the terminal chlorines on each end forming a bond to a copper atom of an adjacent dimer. The copper ions are five-co-ordinate, with a significant distortion from square planar. This distortion is characterized by the bifold angle σ, between the bridging Cu_2Cl_2 plane and the plane of the $CuCl_3$ moiety at the end of the dimer. Magnetic correlations with this structural feature have been given.[14]

Within the dimer, bridging angles (φ) of 95.5 (piperidinium) and 95.8° (piperazinium) are found, which would imply an exchange constant (J/k) of *ca.* −30 K {$K[CuCl_3]$ has $J/k = -28$ K with 95.5°, while $[H_2tatz][Cu_2Cl_6]$ (H_2tatz = 2,4,6-triamino-1,3,5-triazinium) also has $J/k = -28$ K with φ = 95.8°} in the absence of the bifold distortion. Due to the admixture of d_{z^2} character into the magnetic orbital with increasing bifold angle the overlap density at the bridging chlorine decreases, and the antiferromagnetic contributions to the observed coupling constant decrease. A net shift towards ferromagnetism is therefore expected, and indeed observed in the compounds $[NH_3Pr^i][CuCl_3]$ (below the phase transition), $[NH_2Me_2][CuCl_3]$, and 4-benzylpiperidinium trichlorocuprate(II), $[Hbzpip][CuCl_3]$.[14] The $[NH_3Pr^i]^+$ salt, with φ = 95.5 and σ = 19.5°, has $J/k = -14$ K; in the $[NH_2Me_2]^+$ salt the corresponding values are φ = 95.6, σ = 23.6°, and $J/k = 15$ K; and in the Hbzpip salt they are φ = 95.2, σ = 28.7°, and $J/k = 30$ K.[14]

The piperazinium compound has the same type of stacking pattern as the $[NH_3Pr^i]^+$ salt. The molecular dimensions of the two compounds are very similar; bond lengths are the same within 0.02 Å, except for the apical bond which is 2.62 Å in the piperazinium salt, as compared to 2.70 Å in the $[NH_3Pr^i]^+$ salt. However, one major difference occurs in the angles: the *trans* angle between the terminal chlorine and the bridging atom across the copper ion is decreased from 160.5° in $[NH_3Pr^i]$-

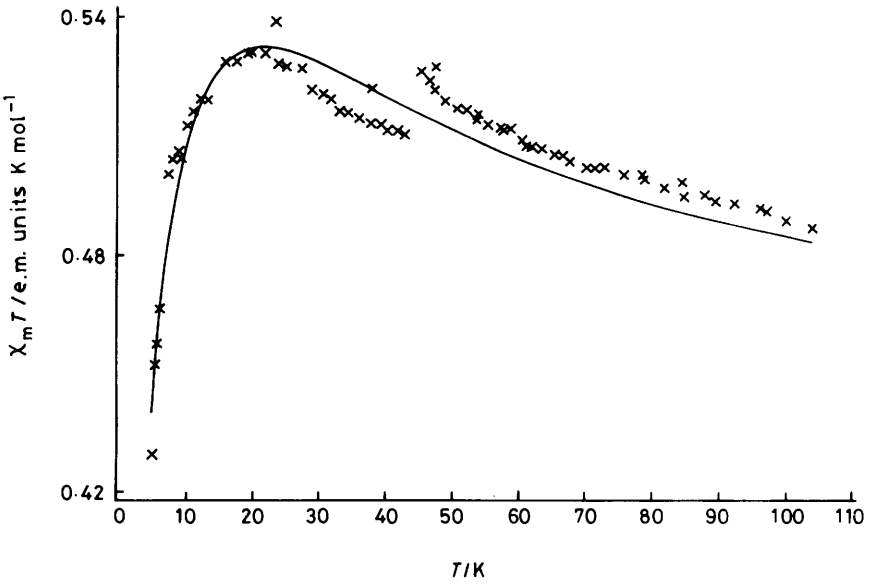

Figure 6. Product of susceptibility and temperature for [Hpip][$CuCl_3$]. (x) Observed values (per mole Cu); (——) calculated curve using J/k = 26 K, g = 2.17, $-ZJ'/k$ = 0.49 K

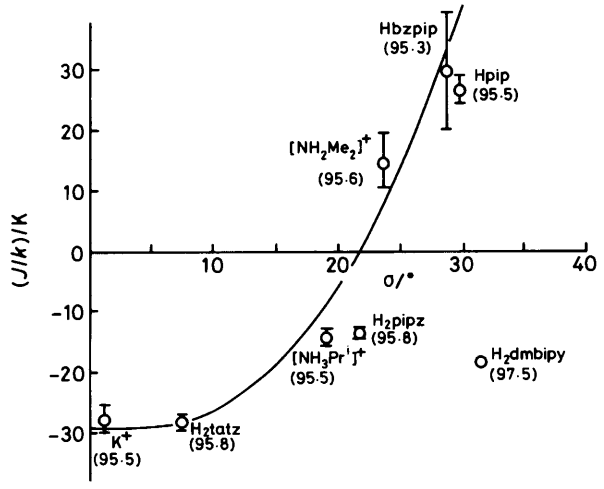

Figure 7. Plot of J/k *vs.* bifold angle (σ) for several $[Cu_2Cl_6]^{2-}$ dimers. The bridging angle (φ) is given in parentheses

[$CuCl_3$] to 156.8°, *i.e.* the bifold angle σ increases from 19.5 to 23.2°. However, the intradimer exchange constant (J/k in the alternating chain model) is only slightly less antiferromagnetic in [H_2pipz][Cu_2Cl_6]: −13.3 *vs.* −14 K in the [NH_3Pr^i]$^+$ salt.

In [Hpip][$CuCl_3$], adjacent dimers are related by a two-fold rotation perpendicular to the intradimer vector. This causes neighbouring units to be oriented approximately at right angles, leading to a zig-zag chain. The same structure type, with the same space group ($C2/c$), was found in dimethylammonium trichlorocuprate(II). Again the geometries of the Hpip and [NH_2Me_2]$^+$ compounds are very similar, the major differences being the *trans* angles, as above: 150.4 *vs.* 156.0°, with corresponding bifold angles of σ = 29.6 and 24.0° for Hpip and [NH_2Me_2]$^+$ respectively. The magnetic data follow the expected trend: an increase in σ leads to increasingly ferromagnetic behaviour, given a comparable bridging geometry.

These results, along with those previously reported, are plotted in Figure 7. With the exception of the [H_2dmbipy]-[Cu_2Cl_6] salt [H_2dmbipy = *N*,*N*′-dimethyl-4,4′-bipyridinium] all have bridging angles, φ = 95.5 ± 0.3° and the trend, exemplified by the solid line, is that the interaction becomes less antiferromagnetic as the distortion from planarity increases. As can be seen, these two compounds complement the previous correlation, although the coupling for the H_2pipz salt appears to be more antiferromagnetic than expected, especially when compared to the [NH_2Me_2]$^+$ salt. It thus may be that some other geometrical parameters, *e.g.* in-plane distortion of bond angles, have additional influence on the amount of exchange coupling. This is borne out by theoretical estimations of the antiferromagnetic exchange contributions to the magnetic exchange utilizing the Hoffmann[27] formulation that $J = J_F - J_{AF}$, with J_F assumed essentially independent of geometry and J_{AF} being proportional to $(\varepsilon_s - \varepsilon_a)^2$, where ε_s and ε_a are the one-electron energies of the symmetric and antisymmetric combinations of the local magnetic orbitals. Based on extended Hückel calculations[28] for the actual observed geometries, we have obtained the energy differences, $\varepsilon_s - \varepsilon_a$, listed in Table 4. The agreement is readily apparent.

It should be noted that the Hoffmann formalism predicts that, as a function of a particular geometrical distortion, J should reach a maximum positive value when $(\varepsilon_s - \varepsilon_a)$ is a minimum and then decrease again as the distortion continues. Such an effect has been observed for the twist distortion.[10b] The continued search for bifolded $[Cu_2Cl_6]^{2-}$ dimers is thus worthwhile to see if a similar effect can be observed.

Electrical Properties and Electro-structural Correlations.— The electrical conductivity at 1 and 60 min after the application of the voltage for both compounds, plotted in Figure 8, exhibits almost linear behaviour as a function of reciprocal absolute temperature. The value of the apparent activation energy for [Hpip][$CuCl_3$] is somewhat higher (0.44 eV) than that of [H_2pipz][Cu_2Cl_6] (0.34 eV). The room-temperature electrical conductivity of [Hpip][$CuCl_3$] is lower (*ca.* 10^{-12} S m^{-1}) than that of [H_2pipz][Cu_2Cl_6] (*ca.* 10^{-9} S m^{-1}), reaching similar values near 100 °C (*ca.* 10^{-7} S m^{-1}). Isochronal and isothermal charging and discharging currents do not exhibit remarkable effects, apart from strong polarization effects, which can even

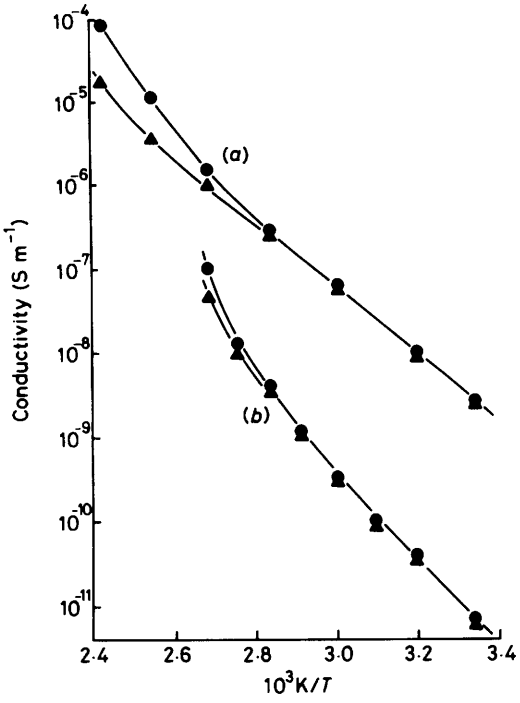

Figure 8. Electrical conductivity after 1 min (●) and 60 min (▲) *vs.* reciprocal absolute temperature for $[H_2pipz][Cu_2Cl_6]$ (*a*) and $[Hpip][CuCl_3]$ (*b*)

reverse the sign of discharging current at the highest temperatures for $[H_2pipz][Cu_2Cl_6]$. This effect increases in intensity and appears at lower temperatures only for samples of $[H_2pipz][Cu_2Cl_6]$ not completely purified and/or dried. No relaxation effects after Fourier transform of the d.c. data were noticed in the ultra-low frequency range.[20]

Dielectric measurements in the frequency range 10^{-2}—10^{-5} Hz at constant temperatures do not show remarkable relaxation effects. The relative dielectric constant regularly decreases with frequency for both compounds, reaching a value of 4 for $[Hpip][CuCl_3]$ and *ca.* 5 for $[H_2pipz][Cu_2Cl_6]$ at 10^5 Hz at room temperature. The loss factor regularly decreases with frequency for both compounds and increases to very high values with decreasing frequencies and increasing temperatures. For both compounds it approaches a unit slope at the highest measurement temperature and lowest frequency.

These results are easily interpreted according to the previously discussed structure of the compounds, thus supplying further evidence for the proposed structures. The behaviour in the a.c. and d.c. experiments suggests a typical ionic mechanism of conduction.[20] Because the compounds were well purified, no charge carriers other than protons can be assumed, according to the structures of Figures 3 and 4. Charge transport can occur *via* the hydrogen bond of the cations in both compounds. This charge transport is more efficient in $[H_2pipz][Cu_2Cl_6]$, since it contains two protonated nitrogen atoms in the piperazinium dications. The presence of otherwise undetectable water and/or hydrogen chloride molecules in $[H_2pipz][Cu_2Cl_6]$ can enhance the phenomenon in this compound, as has been found by chance when it has not been completely purified and/or dried.

Acknowledgements

This work was supported in part by the National Science Foundation (Grants DMR-8219430 and INT-8219425) and in part by a contribution from the Ministero della Pubblica Istruzione (Italy).

References

1 D. W. Smith, *Coord. Chem. Rev.*, 1976, **21**, 93.
2 L. P. Battaglia, A. Bonamartini Corradi, G. Marcotrigiano, L. Menabue, and G. C. Pellacani, *Inorg. Chem.*, 1980, **19**, 125; L. Antolini, G. Marcotrigiano, L. Menabue, and G. C. Pellacani, *J. Am. Chem. Soc.*, 1980, **102**, 1303, 5506; L. Antolini, L. Menabue, G. C. Pellacani, M. Saladini, and G. Marcotrigiano, *Inorg. Chim. Acta*, 1982, **58**, 193.
3 R. L. Harlow, W. J. Wells III, G. W. Watt, and S. H. Simonsen, *Inorg. Chem.*, 1975, **14**, 1786; L. P. Battaglia, A. Bonamartini Corradi, G. Marcotrigiano, L. Menabue, and G. C. Pellacani, *ibid.*, 1979, **18**, 148.
4 H. Place, M.S. Thesis, Washington State University, 1986; H. Place and R. D. Willett, *Acta Crystallogr., Sect. C*, 1987, **43**, 1050.
5 R. D. Willett and U. Geiser, *Croat. Chem. Acta*, 1984, **57**, 737.
6 R. D. Willett, in 'Magneto-Structural Correlations in Exchange Coupled Systems,' eds. R. D. Willett, D. Gatteschi, and O. Kahn, NATO ASI Series, Plenum Press, 1985, p. 389; W. E. Hatfield, *ibid.*, p. 555.
7 L. J. de Jongh and A. R. Miedema, *Adv. Phys.*, 1974, **23**, 1.
8 E. I. Solomon, J. W. Hare, D. M. Dooley, J. H. Dawson, P. J. Stephens, and H. B. Gray, *J. Am. Chem. Soc.*, 1980, **102**, 168.
9 G. Davies and M. A. El-Sayed, *Inorg. Chem.*, 1983, **22**, 1257.
10 (*a*) D. R. Bloomquist and R. D. Willett, *Coord. Chem. Rev.*, 1982, **47**, 125; (*b*) R. D. Willett and U. Geiser, *Inorg. Chem.*, 1986, **25**, 4558.
11 M. Honda, C. Katayama, J. Tanaka, and M. Tanaka, *Acta Crystallogr., Sect. C*, 1985, **41**, 197; B. Scott, personal communication.
12 A. Colombo, L. Menabue, A. Motori, G. C. Pellacani, W. Porzio, F. Sandrolini, and R. D. Willett, *Inorg. Chem.*, 1985, **24**, 2900.
13 U. Geiser, R. D. Willett, M. Lindbeck, and K. Emerson, *J. Am. Chem. Soc.*, 1986, **108**, 1173.
14 S.O'Brien, R. M. Gaura, C. P. Landee, B. L. Ramakrishna, and R. D. Willett, *Inorg. Chim. Acta*, in the press; R. D. Willett, T. Grigereit, K. Halvorson, and B. Scott, *Ind. Acad. Sci.*, 1987, **98**, 147.
15 D. B. Brown, V. H. Crawford, J. W. Hall, and W. E. Hatfield, *J. Phys. Chem.*, 1977, **81**, 1303.
16 R. L. Powell, M. D. Bunch, and R. J. Corruccini, jun. (ed.), *Nat. Bur. Stand., Spec. Publ.*, No. 300, 1968, vol. 2, pp. 319—321.
17 F. Sandrolini and P. Cremonini, *Mater. Plast. Elastomeri.*, 1979, 405.
18 F. Sandrolini and P. Manaresi, Proc. 26th Int. Symp. Macromol. IUPAC, Mainz, 17—21 September, 1979, eds. I. Ludenwald and R. Weis, vol. 3, p. 1463.
19 F. Sandrolini, *J. Phys. E.*, 1980, **13**, 152.
20 F. Sandrolini, in 'Macromolecole: Scienza e Tecnologia,' ed. F. Ciardelli, Pacini, Pisa, 1985, sect. 5, vol. 2.
21 'User Manual for Philips PW1100,' Philips, Eindhoven, The Netherlands.
22 'International Tables for *X*-Ray Crystallography,' Kynoch Press, Birmingham, 1974, vol. 4, pp. 99—100 and 149—150.
23 G. M. Sheldrick, 'SHELX 76, program system for crystal structure determination,' University of Cambridge, 1976.
24 B. J. Hathaway, *Coord. Chem. Rev.*, 1982, **41**, 423.
25 J. W. Hall, W. E. Marsh, R. R. Weller, and W. E. Hatfield, *Inorg. Chem.*, 1981, **20**, 1033.
26 C. Chow, R. D. Willett, and B. C. Gerstein, *Inorg. Chem.*, 1975, **14**, 205.
27 P. J. Hay, S. C. Thibeault, and R. Hoffmann, *J. Am. Chem. Soc.*, 1978, **97**, 4884.
28 R. Hoffmann, *J. Chem. Phys.*, 1963, **39**, 1397.

Received 2nd *July* 1986; *Paper* 6/1329